Supplemental Information

Nuclear mTOR acts as a transcriptional integrator of the androgen-signaling pathway in prostate cancer

Étienne Audet-Walsh, Catherine R. Dufour, Tracey Yee, Fatima Z. Zouanat, Ming Yan, Georges Kalloghlian, Mathieu Vernier, Maxime Caron, Guillaume Bourque, Eleonora Scarlata, Lucie Hamel, Fadi Brimo, Armen G. Aprikian, Jacques Lapointe, Simone Chevalier, and Vincent Giguère

Document S1. Supplemental Experimental Procedures, Figures S1-S7, and Tables S2-S5.

Audet-Walsh_Figure S1

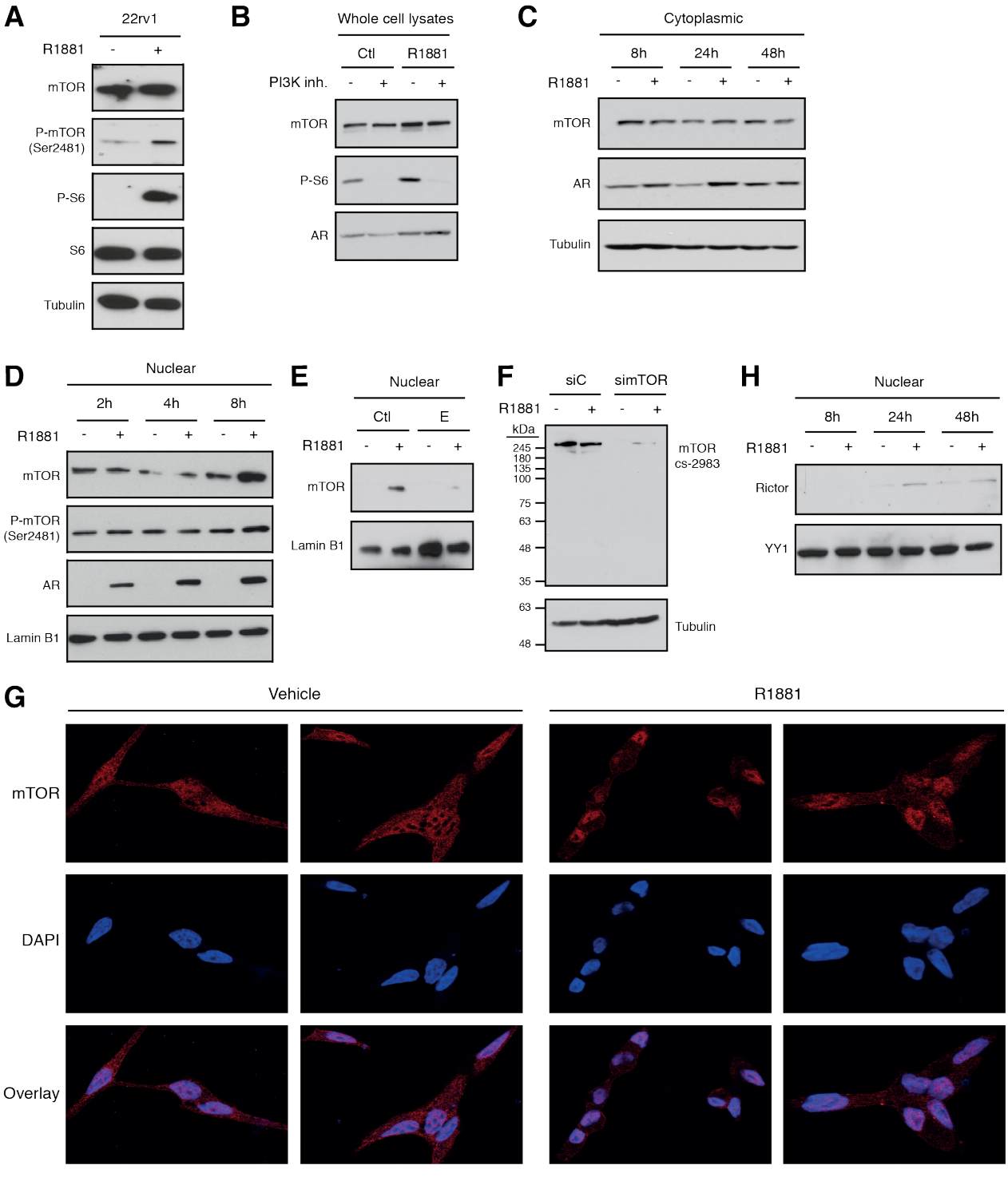

Figure S1. **AR signalling controls mTOR nuclear levels in PCa cells.**
(A) Western blot analysis of whole cell lysates from 22rv1 cells treated with R1881 or vehicle for 48h. Tubulin levels are shown as a loading control. (B) Whole cell lysates of LNCaP cells following a 24 h stimulation with R1881, with or with the PI3K inhibitor, GDC-0941. (C) Time-course of androgen-induced mTOR cytoplasmic fraction in from LNCaP cells. Tubulin levels are shown as a loading control. (D) Time-course of androgen-induced mTOR nuclear accumulation in LNCaP cells. Lamin B1 levels are shown as a nuclear loading control. (E) Western blot analysis of nuclear fractions of LNCaP cells treated with R1881 or vehicle for 48 h, with or without co-treatment with enzalutamide. Lamin B1 levels are shown as a loading control. (F) Specificity of mTOR antibody evaluated in LNCaP cells treated with siRNAs against mTOR, with or without 24 h treatment with R1881. (G) Immunofluorescence of mTOR in LNCaP cells treated with R1881 or vehicle for 48h. (H) Time-course of rictor nuclear accumulation following R1881 stimulation in LNCaP cells. YY1 levels are shown as a nuclear loading control.

Audet-Walsh_Figure S2

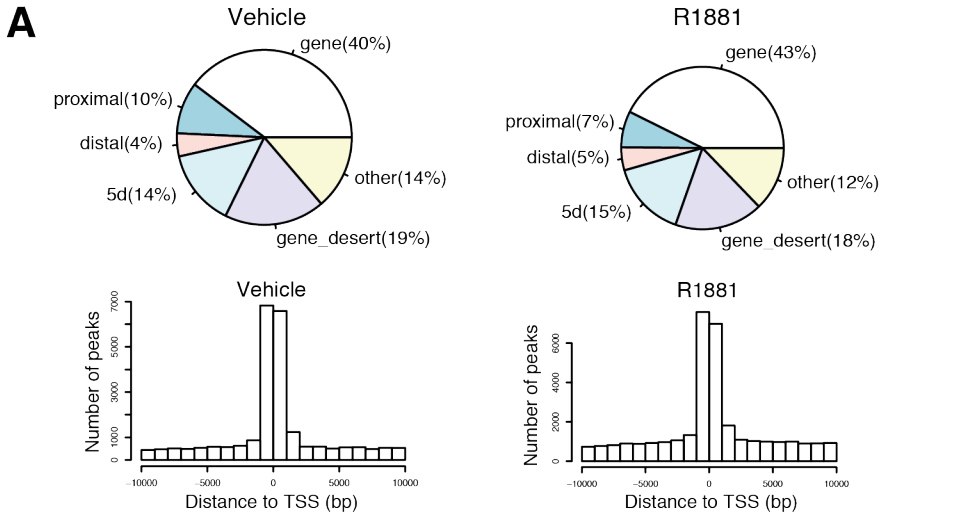

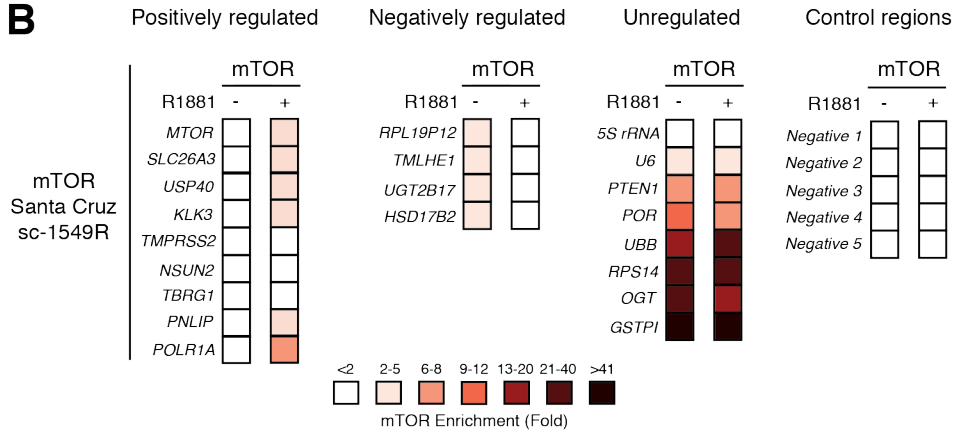

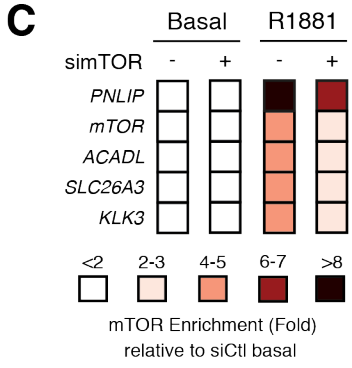

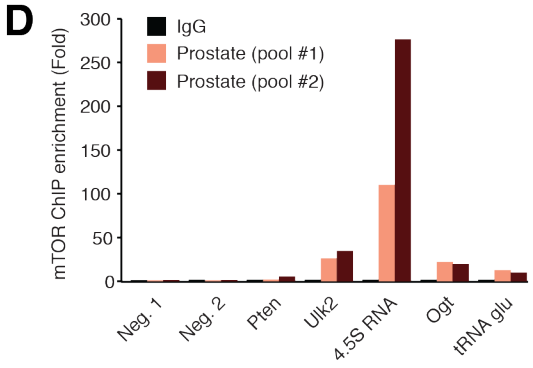

Figure S2. AR signalling controls mTOR nuclear activity in PCa cells. (A) Pie charts and histograms illustrating the mapping of mTOR DNA binding across the genome and relative to the TSS of genes identified by ChIP-seq in LNCaP cells treated with or without R1881 for 48 h. (B) Validation of mTOR DNA binding with a second antibody by ChIP-qPCR in LNCaP cells ± R1881 for 48 h. Relative fold enrichment was normalized over 2 negative regions and are shown relative to IgG (set at 1). Results are shown as the average of 3 independent experiments. (C) Validation of mTOR ChIP using control siRNAs or siRNAs against mTOR. Results are shown as the average of 3 independent experiments. Refer to Fig. S1F for residual mTOR levels upon inhibition with siRNAs. (D) DNA binding of mTOR in the mouse prostate. ChIP-qPCR assays were performed using mTOR or IgG antibodies on pools of the different mouse prostatic lobes.

Audet-Walsh_Figure S3

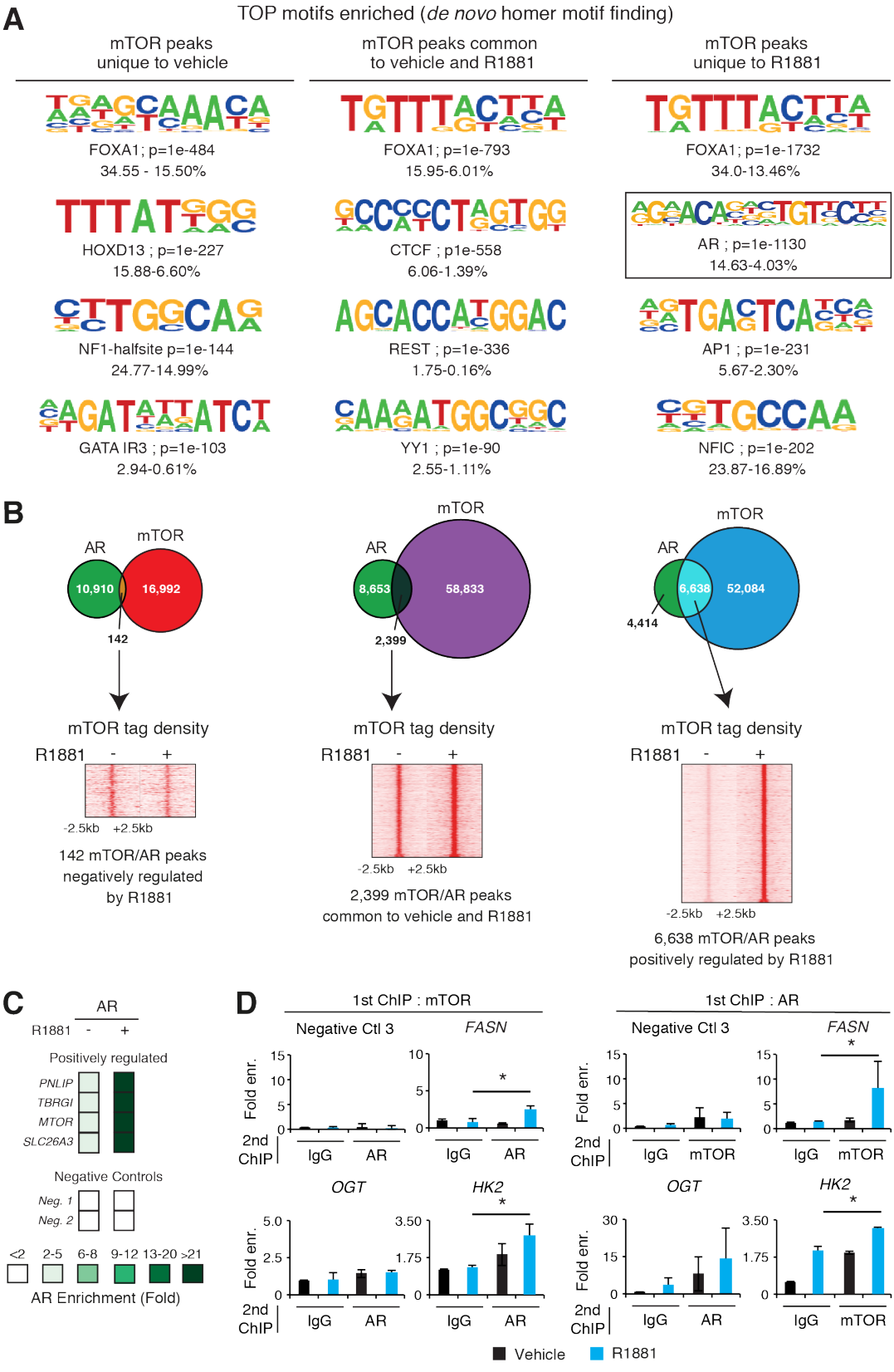

Figure S3. **AR reprograms mTOR DNA binding in PCa cells.** (A) *De novo* DNA motif enrichment analysis of mTOR ChIP-seq data in LNCaP cells. Proportion of peaks containing the motifs compared to background are indicated below the transcription factors and *p* values associated with each motif are shown. (B) Venn diagrams illustrating the overlap between AR and mTOR ChIP-seq datasets distinguished by the effect of R1881. Heatmaps showing the signal intensity of mTOR binding for the common AR-mTOR bound peaks differentially affected by R1881 are shown. (C) ChIP-qPCR of AR in LAPC4 cells at mTOR DNA binding sites as shown in Figure 1. Results are shown as the average of 4 independent experiments. D) ChIP-reChIP analysis shows co-recruitment of AR and mTOR to the same genomic regions following androgen treatment (see also Figure 2F). Results are shown as the average of 2 independent experiments.

Audet-Walsh_Figure S4

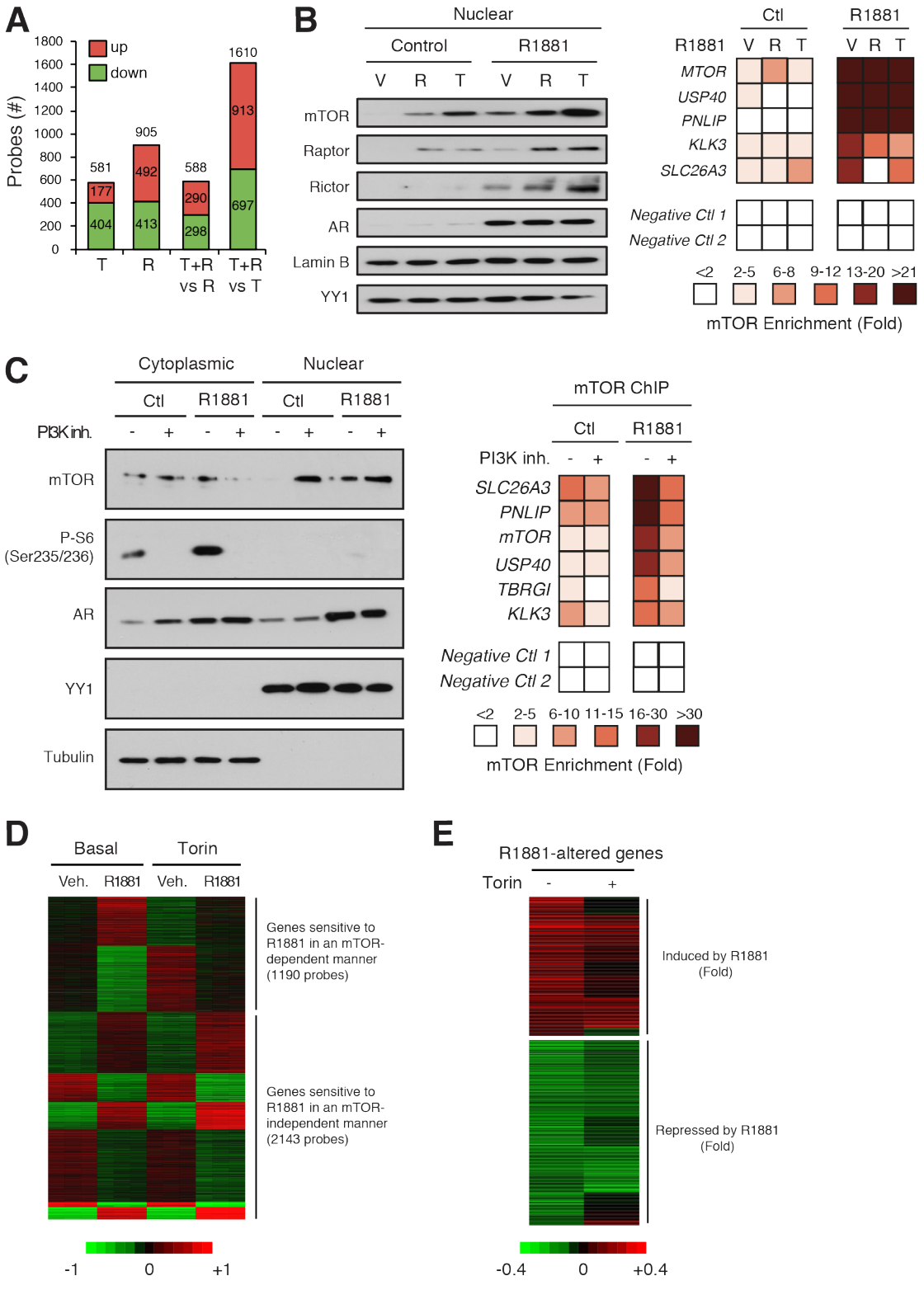

Figure S4. mTOR activity is essential for specific transcriptional program in PCa cells. (A) Number of microarray probes significantly modulated by R1881 (R), torin 1 (T), or both in LNCaP cells with a *p* under 0.001 and a fold-change of 1.5 or more. (B) Western blot analysis (left) of nuclear fractions of LNCaP cells treated with R1881 or vehicle for 48h, with or without co-treatment with rapamycin (R) or torin 1 (T). Lamin B1 is shown as a loading control. mTOR DNA binding (right) in LNCaP cells following a 48 h treatment. ChIP-qPCR values represent the average of 3 independent experiments. (C) Western blot analysis (left) of cytoplasmic and nuclear fractions of LNCaP cells treated with R1881 or vehicle for 48 h, with or without co-treatment with the PI3K inhibitor, GDC-0941. YY1 and tubulin are shown as nuclear and cytoplasmic loading controls, respectively. DNA binding (right) assays in LNCaP cells following a 24 h treatment with R1881 and/or the PI3K inhibitor. ChIP-qPCR values represent the average of 2 independent experiments. (D) Heatmaps of clusters of genes modulated by R1881 in an mTOR-dependent (sensitive; upper part) or mTOR-independent (insensitive; bottom part) manner. For clustering analysis, all probes significantly modulated by R1881 with a $p < 0.01$ were used for initial analysis (see M&M for more details). (E) Probes identified in panel (D) to be AR- and mTOR-dependent ("sensitive probes") are shown using fold change following R1881.

Audet-Walsh_Figure S5

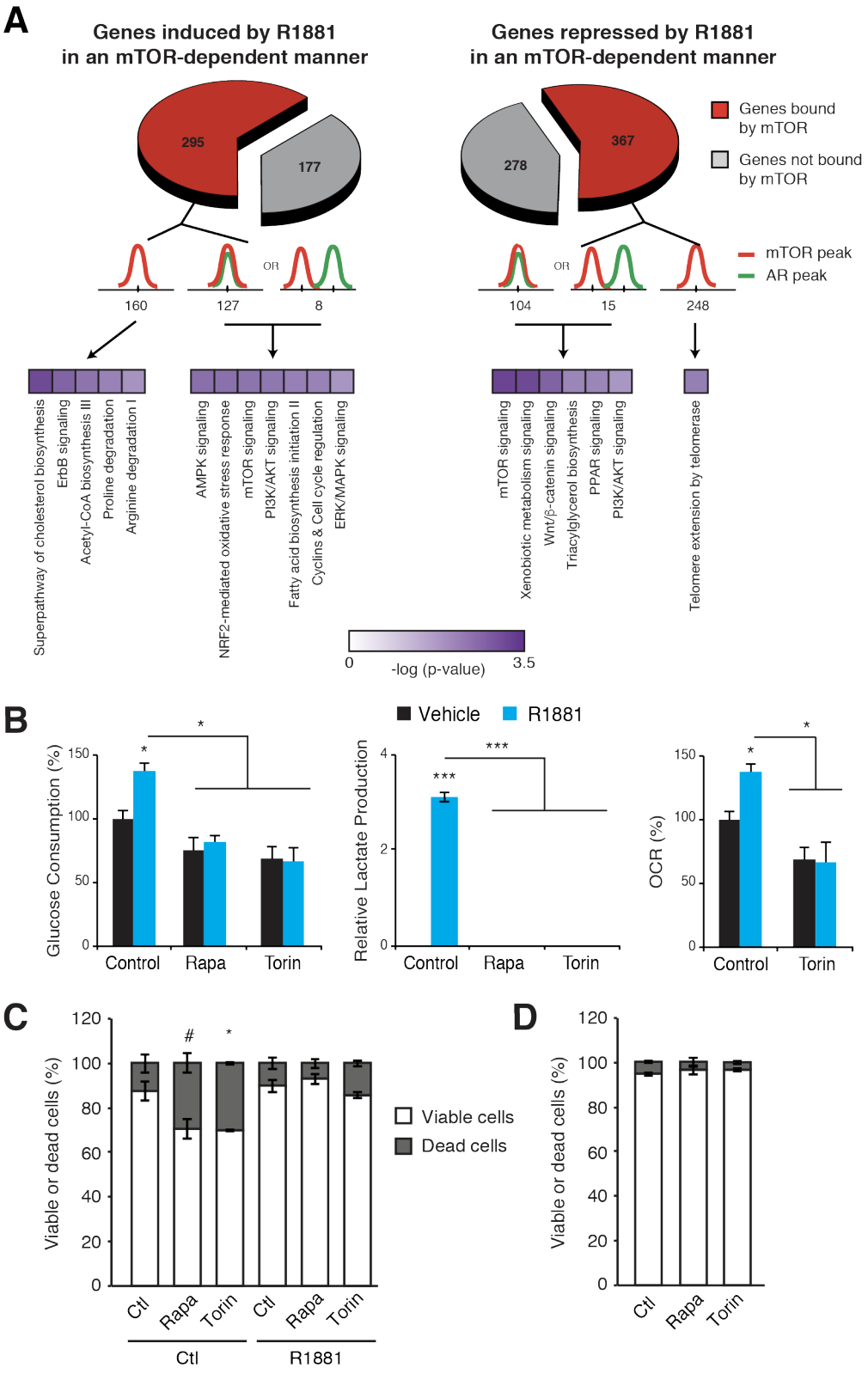

Figure S5. mTOR is essential for androgen-mediated reprogramming of PCa cell metabolism. (A) Functional genomics crosstalk of AR and mTOR in PCa cells. Genes regulated by AR activation and for which mTOR inhibition blocked or impaired this regulation (torin 1 treatment) are shown. Intersection of these regulated genes with mTOR and AR ChIP-seq data are shown along with enrichment of these gene subsets within biological pathways determined by IPA analysis. (B) Measurement of glucose consumption, lactate production, and oxygen consumption rates (OCR) in LAPC4 cells treated with or without R1881 and mTOR inhibitors. Values represent mean ± SEM of 3 independent experiments. (C) Cell survival analysis following a 4 d treatment with rapamycin, torin 1, and/or R1881 in LNCaP cells. One representative experiment performed in triplicate is shown. (D) Cell survival analysis following a 2 d treatment with rapamycin or torin 1 in DU145 cells (n=5). *$p < 0.05$, #$p < 0.10$, by Student's t-test.

Audet-Walsh_Figure S6

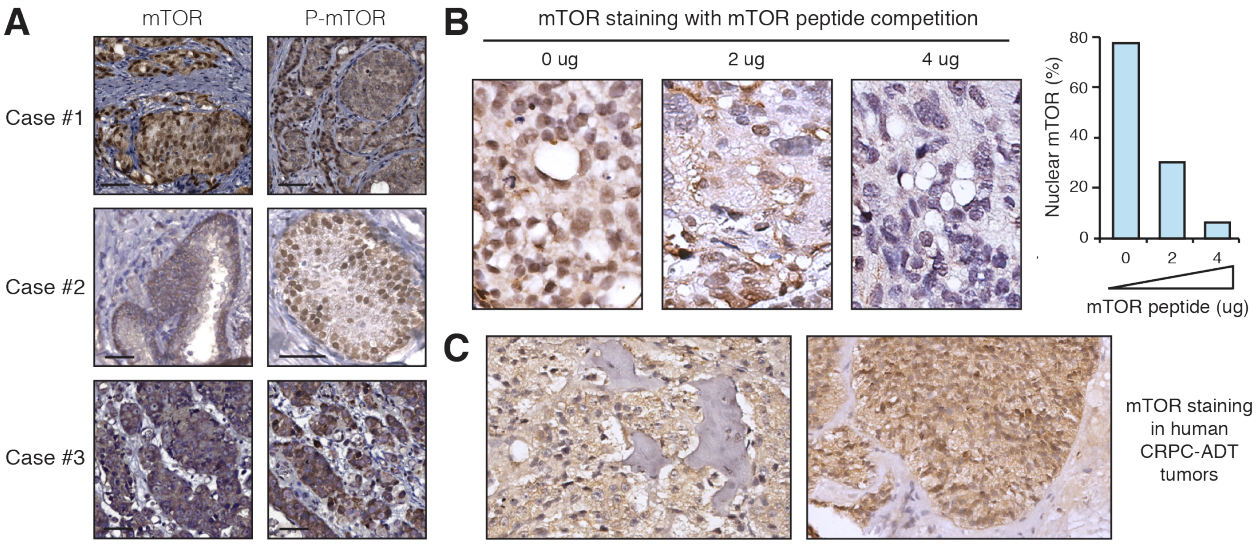

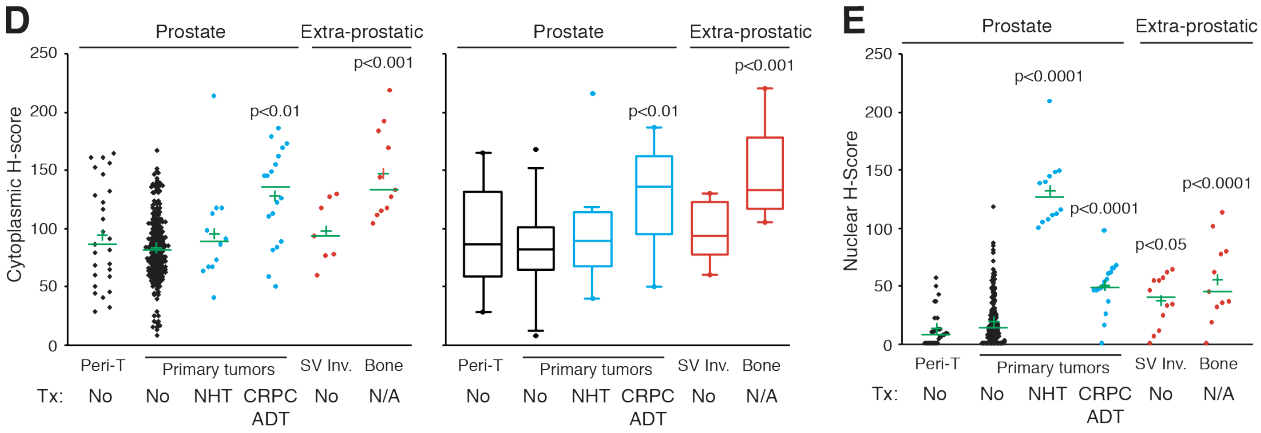

F

Distribution of cases based on the percentage of positively stained cell nuclei

Patient specimens	Number of cases (n)	<10%		10-30%		>30%	
		n	%	n	%	n	%
Peri-tumoral	30	15	50	12	40	3	10
Primary (unt.)	232	82	35	118	51	32	14
Primary (NHT)	12	0	0	3	25	9	75
Primary (CRPC-ADT)	18	1	6	5	28	12	67
Seminal vesicle Inv.	12	2	17	4	33	6	50
Bone	11	1	9	4	36	6	55

Chi-square test p<0.0001

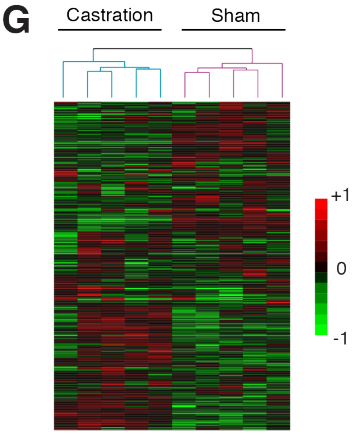

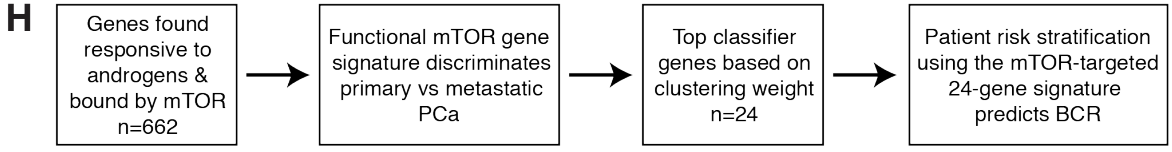

Figure S6. Levels of nuclear mTOR protein and its downstream transcriptional gene signature both correlate with PCa progression. (A) Representative staining using mTOR and phospho-mTOR antibodies from Cell Signaling Technology in 3 PCa patient samples to validate the detection of nuclear mTOR in the TMA analysis using the mTOR antibody from Abcam. Scale bar representing 50 *u*m. (B) Validation of the mTOR antibody specificity using an mTOR peptide in a competition assay in samples from the same CRPC tumor; quantification is shown (right). (C) Additional pictures of mTOR staining in CRPC-ADT tumor samples. Cytoplasmic (D) and nuclear (E) H-score of mTOR staining of peri-tumoral, primary PCa tumors and metastatic lesions. Peri-T, peri-tumoral; SV Inv., seminal vesicle invasion; Tx, treatment. Green line and plus sign represent median and average values, respectively. ANOVA was used to assess significant trends and post-hoc analysis was used to determine which groups were significantly different. *P* values indicate significant differences compared to both peri-tumoral and untreated (unt) primary PCa tumors. (F) Contingency table of the proportion of cells with positive nuclear mTOR staining across sample types. (G) Unsupervised hierarchical cluster analysis with an mTOR-targeted gene signature discriminates between castration and control LuCaP35 xenografts (Sun et al. 2012). (H) Schematic depicting the derivation of the functional prostate cancer mTOR-targeted gene signatures.

Audet-Walsh_Figure S7

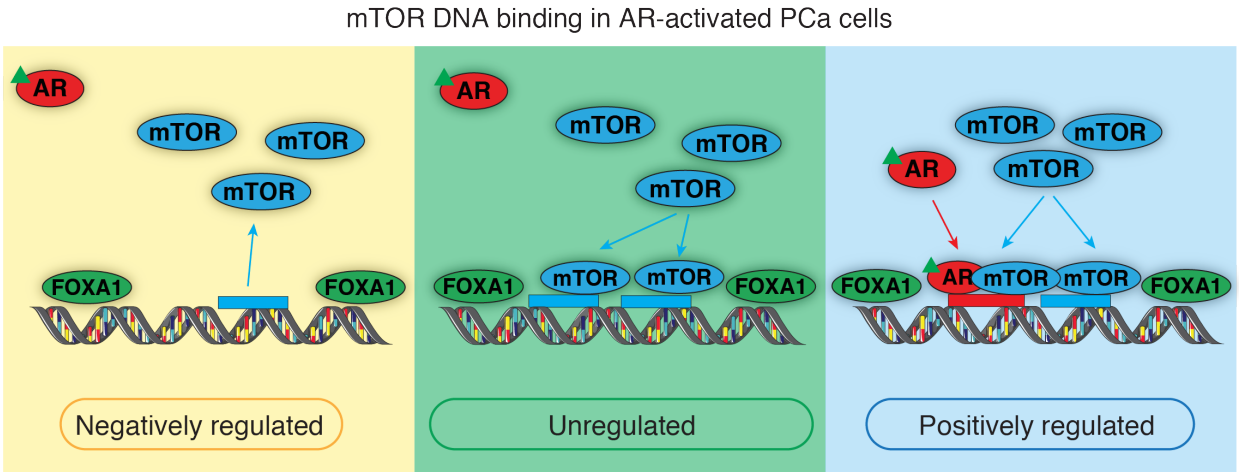

Figure S7. Working model for mTOR DNA binding upon AR activation. FOXA1 serves as a pioneer factor for mTOR, both in absence and presence of androgen. However, upon AR activation, mTOR binding is lost at some sites (binding events negatively regulated by androgen). Most DNA binding sites bound by mTOR in absence of androgen remains bound by mTOR upon AR activation, with even a slight increase in DNA average binding signal, possibly reflecting increased nuclear mTOR levels. Finally, AR binding to DNA allows recruitment of mTOR to DNA binding sites positively regulated by androgen.

Table S1. Functional IPA and GO cellular component analyses along with the identified mTOR-targeted multi-gene signatures determined from R1881- and torin 1-responsive genes bound by mTOR from ChIP-seq analysis in LNCaP cells.

See Excel file.

Table S2. Characteristics of the human PCa cell lines used in this study.

Cell Line	AR status	PTEN status
LNCaP	+ (mutation T878A)	-
22rv1	+ (mutation H875Y)	Wild type
LAPC4	+	Wild Type
PC3	-	-
DU145	-	Wild type

This table is based on several reports, including (Vlietstra et al. 1998; Wu et al. 1998; Mehrian-Shai et al. 2007; Gravina et al. 2011; Watson et al. 2015). See also the recent review by Watson et al. for the various PCa cell line descriptions and model comparisons (Watson et al. 2015).

Table S3. Human qRT-PCR primers.

Primer	Sequence
TBP forward	TGCCACGCCAGCTTCGGAGA
TBP reverse	ACCGCAGCAAACCGCTTGGG
PUM1 forward	ACGGATTCGAGGCCACGTCC
PUM1 reverse	CATTAATTACCTGCTGGTCTGAAGGA
ATP5L forward	CTGACCTTGGAAGTGGGACG
18S forward	GTCTGTGATGCCCTTAGATG
18S reverse	AGCTTATGACCCGCACTTAC
ATP5L reverse	AAGTCACAGCAGCGTTCACC
ACACB forward	TTGCAGTCCCCAGAGTAAGC
ACACB reverse	AGAAAATCACTTTATTCCTGCCGC
NDUFA6 forward	AAGCTACTTCTACCGCCAGC
NDUFA6 reverse	AATTGGTGCACAGTGTTCGG
ENO1 forward	GTGGGGCTCGCCTTAGC
ENO1 reverse	CATGGTGAACTTCTAGCCACT
ALDH1A3 forward	TCGACCTGGAGGGCTGTATT
ALDH1A3 reverse	CACGACGTTGTCATCTGTGG
FASN forward	CTGCCAGAGTCGGAGAACTT
FASN reverse	TTGATGCCTCCGTCCACGAT
HK2 forward	GCTGTGGTGGACAGGATACGAGAA
HK2 reverse	CGCCGCCCCCTTCCCGCTGCCATC
PDHX forward	TCCCGGGAGGTGATCCCATTA
PDHX reverse	ATGCATCTCCAGCACTCACC
PFKP forward	GGAAGTTCCTGGAGCACCTC
PFKP reverse	CCCTGGTAGCCCTCGTAGAT
PFKFB2 forward	AGGCAGGGAGGGATCTTAGG
PFKFB2 reverse	CATGTAGGAGGCCCATGAACA

Table S4. Human ChIP-qPCR primers.

Primer	Sequence	Description
KLK3 #1 forward	TGCCACTGGTGAGAAACCTGAGAT	*KLK3* (PSA) enhancer at -4 kb
KLK3 #1 reverse	TCAGAGACAAAGGCTGAGCAGGTT	*KLK3* (PSA) enhancer at -4 kb
KLK3 #2 forward	AGGTGGATCAGCAGTCCGACATAA	*KLK3* (PSA) enhancer at -12.5 kb
KLK3 #2 reverse	CACACAGTGGTTTGCGTCAATGCT	*KLK3* (PSA) enhancer at -12.5 kb
Negative 1 forward	GAAGCCCATTTTCCCTCCCA	Negative control
Negative 1 reverse	CAATGGGGCTGAAGCACAAC	Negative control
Negative 2 forward	CCCCTGTACATGGTGAACACT	Negative control
Negative 2 reverse	GGCACCACGGTAGTACGAAA	Negative control
EP300 forward	AATGAATTGGCGAGAGGTTG	Negative control
EP300 reverse	AAACCTCACTCCTGCCACAC	Negative control
Chr.17 #2 forward	ACATGTTGGGACTGTTGCCA	Negative control
Chr.17 #2 reverse	GTTCCACCTCAGACTGCACA	Negative control
Chr.17 #3 forward	CTACTCCTGGGGTGCTGGA	Negative control
Chr.17 #3 reverse	AGGGGACTGGCTCTTCTTCA	Negative control
HPCAL4 forward	TTTGGGTGAGGACAGAGGTC	Negative control
HPCAL4 reverse	CCAGCCACAAAGAAGATGGT	Negative control
NEGATIVE 5	CCCCTGTACATGGTGAACACT	Negative control
NEGATIVE 5	GGCACCACGGTAGTACGAAA	Negative control
POR forward	GCCGTACCAAGAGCGCAAAT	mTOR DNA binding site
POR reverse	GCCGCGAAAGATAGCACTCA	mTOR DNA binding site
UBB forward	TTTCCAGAGCTTTCGAGGAAGG	mTOR DNA binding site
UBB reverse	CGTCACTTATCACCCCTCACG	mTOR DNA binding site
RSP14 forward	CTAGACAGACTTCCGCCATCC	mTOR DNA binding site
RSP14 reverse	GCCAAAGTAAGTGATTACGGTGT	mTOR DNA binding site
GSTPI forward	TACCTTCGCCTCGGTAGTTC	mTOR DNA binding site
GSTPI reverse	CCCTGTCCCTGAACTTCGACT	mTOR DNA binding site
OGT forward	TACCTTCGCCTCGGTAGTTC	mTOR DNA binding site
OGT reverse	CCCTGTCCCTGAACTTCGACT	mTOR DNA binding site
SLC26A3 forward	AGGATGTGGGCATCTTTGGG	mTOR DNA binding site
SLC26A3 reverse	GAGATAGCAGCCAGGCACAA	mTOR DNA binding site
POLR3E forward	GTAGAAACCGGGTGACGCTC	mTOR DNA binding site
POLR3E reverse	CTAAGTACCGACCTCCAGACC	mTOR DNA binding site
NDUFA7 forward	ATCTTCCGTCCGCGATACTG	mTOR DNA binding site
NDUFA7 reverse	ATACCACGCCGCGTCTTTC	mTOR DNA binding site
mTOR forward	AGAGAAGGCTTGCTCACTCTTC	mTOR DNA binding site
mTOR reverse	AACATAAAACACATCTGCACTTCCA	mTOR DNA binding site

ACADL forward	CTTGAGCCCTGAAGACTGGG	mTOR DNA binding site
ACADL reverse	ATGTCCCCAGGTACTCTCCC	mTOR DNA binding site
USP40 forward	GGTGCTAGCGCCATGTGTC	mTOR DNA binding site
USP40 reverse	AATAATATTCCAAAGTGGCTGGACC	mTOR DNA binding site
TMPRSS2 forward	TGAGACTAGCCTGGACACCA	mTOR DNA binding site
TMPRSS2 reverse	AAGCTCACTGCAGCCTCAAA	mTOR DNA binding site
TBRG1 forward	ACACAGGCCAAGAACCAGAA	mTOR DNA binding site
TBRG1 reverse	AGCACTGGATTGGGGGTTTAG	mTOR DNA binding site
PNLIP1 forward	CCAGTTGCCTAGAGTACACAGA	mTOR DNA binding site
PNLIP1 reverse	GTGAGTAACCGAACGCCGA	mTOR DNA binding site
TMLHE1 forward	ACTCATACAGTCTTCTGCACAAAT	mTOR DNA binding site
TMLHE1 reverse	TCTACGTTTGTTGCTTTCGAGT	mTOR DNA binding site
UGT2B17 forward	GGAAGGTTGAGGCAAGTGGA	mTOR DNA binding site
UGT2B17 reverse	ACCTCCACCCTCTAGGTTCA	mTOR DNA binding site
HSD17B2 forward	ACAAGGAAATGCGTCCAAAGTC	mTOR DNA binding site
HSD17B2 reverse	CCTGGGTAACCTTTGTGGTCTA	mTOR DNA binding site
RPLP19P12 forward	CACCAATGGTAACAAATGCCCA	mTOR DNA binding site
RPLP19P12 reverse	AGTGCTTGGTACATAGTAAATGCT	mTOR DNA binding site
NSUN2 forward	GCAACAGGAAAACAGCACATAAT	mTOR DNA binding site
NSUN2 reverse	AATGGTATAGCAACCATTTGTCCG	mTOR DNA binding site
U6 forward	TTCTTGGGTAGTTTGCAGTTTT	mTOR DNA binding site
U6 reverse	TGTTTCGTCCTTTCCACAAG	mTOR DNA binding site
5S rRNA forward	GGCCATACCACCCTGAAC	mTOR DNA binding site
5S rRNA reverse	GCGGTCTCCCATCCAAGTA	mTOR DNA binding site
ADPGK forward	CTCAGGAGTTCGAGACCAGC	mTOR DNA binding site
ADPGK reverse	ATCCTTCTGCCTCAGCCTCT	mTOR DNA binding site
ALDH1A3 forward	CTCTGCTGTGGGAACACCAT	mTOR DNA binding site
ALDH1A3 reverse	GTCTGCCACTGTCCCATCTC	mTOR DNA binding site
HK2 forward	GCTCCAAGCTTCCTGACAGT	mTOR DNA binding site
HK2 reverse	GCCGATGGGATGAAAACGAC	mTOR DNA binding site
HK1 forward	ACAACTGGGACCACAGCAAA	mTOR DNA binding site
HK1 reverse	CCTCCAGGAGCTTTAGTGCC	mTOR DNA binding site
PDHX forward	TAGAGTGAGGGGGCGGTAAA	mTOR DNA binding site
PDHX reverse	CCAAGAGCCCATTCTCTGCT	mTOR DNA binding site
PFKFB2 forward	ATGTTTGCACACTGGCTTGC	mTOR DNA binding site
PFKFB2 reverse	ATTCCTGCACCTGCAACTGT	mTOR DNA binding site
SLC2A1 forward	AACAATGCCTTTCATGCCGA	mTOR DNA binding site
SLC2A1 reverse	GGGCAACATAGCAAGACCCT	mTOR DNA binding site
LDHB forward	CATTCCCCAGGCCCTTACTG	mTOR DNA binding site
LDHB reverse	CGGTGCCCTGAGGAAAAGAT	mTOR DNA binding site

*LDHD*1 forward	AACAGGCAAGTTCGTCTCGTC	mTOR DNA binding site
LDHD1 reverse	GGGTAACCTCTGTTGCAATAACTA	mTOR DNA binding site
LDHD2 forward	GAGCTTCATGATTTCGGGCG	mTOR DNA binding site
LDHD2 reverse	GAGCCCGTCTTGAGACCTTG	mTOR DNA binding site
ACACB forward	GGCCTAGCCAAGGTAGTCATC	mTOR DNA binding site
ACACB reverse	CACTGTGTAGCCCAGTAAAGGT	mTOR DNA binding site
FASN forward	AAGTGCCTAGGGCCCTTTTT	mTOR DNA binding site
FASN reverse	GAAGACTGGATGTGGTGGCA	mTOR DNA binding site
AMACR #2 forward	AGTCATCTCATCACGCCACC	mTOR DNA binding site
AMACR #2 reverse	GGTGCTGGAGACATTAGGCT	mTOR DNA binding site
SOAT1 forward	TGCGTGCACAGATTAGATTCTT	mTOR DNA binding site
SOAT1 reverse	TGCAGGAGATTCAGAAATGCT	mTOR DNA binding site
PFKP #3 forward	GCCCAGCTTCTCCTGTCATT	mTOR DNA binding site
PFKP #3 reverse	GTCCATTCTGGCCCATGTGA	mTOR DNA binding site
ENO1 #2 forward	GGGGCTTATGTCTTGCCAGT	mTOR DNA binding site
ENO1 #2 reverse	AGAGGTTTCCATTGGTTACTTGGT	mTOR DNA binding site
NDUFA6 forward	CACACAGCTAGTTGAGGGCA	mTOR DNA binding site
NDUFA6 reverse	CGGGATTTCACCGTGTTAGC	mTOR DNA binding site
ATP5L #4 forward	TTCAGTTGTCTTCTCAGTGGCAA	mTOR DNA binding site
ATP5L #4 reverse	AACTCAAACACAGCAAAATAGGCT	mTOR DNA binding site
PDHX #2 forward	GTCGCAGAAGTCTAGGAGGTTGAA	mTOR DNA binding site
PDHX #2 reverse	GTATATGACCCAGGGTGGAGAAGAA	mTOR DNA binding site
PFKFB2 #2 forward	TACCAAGCAACAGTGCCACC	mTOR DNA binding site
PFKFB2 #2 reverse	TACAGTCGCCGGCAAATCAT	mTOR DNA binding site

Table S5. Mouse ChIP-qPCR primers.

Primer	**Sequence**	**Description**
Negative 1 forward	TTGGCATTGATATTGGGGGTGGGAGCAACT	Negative control
Negative 1 reverse	GACTTCTTACTTTGACGCTTTCCTCCATCG	Negative control
Negative 2 forward	CCAAGCACAAATATCTAATCACCCTTTC	Negative control
Negative 2 reverse	CTTCTTGATAGGTTTATGGGTTGGGC	Negative control
Pten forward	CCTCGCCTTTGAGCCCTCC	mTOR DNA binding site
Pten reverse	CCCCCAATCCCCACTTCGT	mTOR DNA binding site
Ulk2 forward	TGCGCCCCAGTCCTGCTCCC	mTOR DNA binding site
Ulk2 reverse	AGCCCGCCGCCCGTTCCTAA	mTOR DNA binding site
4.5S RNA forward	AGAACCGGCGAGCGTTGCTG	mTOR DNA binding site
4.5S RNA reverse	AGGTTGACGGTGCGGTTTGG	mTOR DNA binding site
Ogt forward	TTGCCCTTCCGCCTTGCTCT	mTOR DNA binding site
Ogt reverse	GGAGGTAGCGCGTAACAAGA	mTOR DNA binding site
tRNA glu forward	CAAAGACAGCCTGCCGAAAC	mTOR DNA binding site
tRNA glu reverse	AACCGCTAGACCATGTGGGA	mTOR DNA binding site

Primers were from data published by Chaveroux et al. (Chaveroux et al. 2013).

Supplemental Experimental Procedures

Cells

Cell viability was assessed in LNCaP cells following 4 d treatment with R1881, rapamycin, and/or torin 1, using Trypan blue (Gibco), as per the manufacturer's recommendation. For immunofluorescence studies, cells were plated on coverslips coated with poly-L-lysine in media with CSS. After 48h (steroid deprivation), fresh media was added, with or without R1881 stimulation. After treatment, cells were fixed with 4% paraformaldehyde in PBS for 10 min at room temperature. After washing with PBS, cells were permeabilized for 5 min with 0.5% Triton X-100 in PBS-BSA 3%. Then, cells were washed three times for 10 minutes in PBS/BSA and incubated overnight with the primary antibodies diluted in PBS/BSA. After incubation with mTOR antibody (N-19 Santa Cruz), cells were washed three times in PBS/BSA and incubated with the appropriate secondary antibody combination for 1h at room temperature. Finally, cells were rinsed three times with PBS alone and once with PBS containing 300 mM DAPI for 10 min.

Protein Analysis

Cell were lysed with buffer K supplemented with protease and phosphatase inhibitors for whole cell lysates or separated into nuclear and cytoplasmic fractions by differential centrifugation as described previously (Chaveroux et al. 2013). For nuclear and cytoplasmic extracts, after 48 h treatment or as indicated, cells were lysed with Harvest buffer (Hepes 10 mM, NaCl 50 mM, Sucrose 0.5M, EDTA 10 mM, Triton X100 0.5%) and incubated on ice for 5 min. Whole cell lysates were then centrifuged at 800*g* for 10 min. The supernatant was removed and centrifuged at 10,000*g* for 15 min at 4ºC to obtain the cytosolic fraction. The nuclear pellet was washed twice with buffer A (Hepes 10 mM, KCl 10 mM, EDTA 0.1 mM, EGTA 0.1 mM) and centrifuged at 800*g* for 10 min at 4ºC. The final pellet was resuspended with High Salt buffer (Hepes 25 mM, NaCl 0.4M, MgCl2 1.5 mM, EDTA 0.2 mM, NP40 1%) and rotated at 4ºC for 60 min. Finally, nuclear extracts were centrifuge at 10,000*g* for 15 min at 4ºC. The supernatants, containing nuclear proteins, were collected and each fraction was used for Western blotting. Antibodies used for protein detection: AR (Santa Cruz, sc-816), P-S6 (S235/236, Cell Signaling, 2211), S6 (Santa Cruz, sc-74459), P-Akt (9271S CST; S473), mTOR (Cell Signaling Technology, 2983), P-mTOR on S2448 (Cell Signaling Technology, 2971), Lamin B1 (Cell Signaling Technology, 12586), anti-α-Tubulin (Cederlane, CLT-9002), P-p70 S6K (T389; Cell Signaling Technology, 9205), and Raptor (Cell Signaling Technology, 2280).

For AR visualization by Western Blot following co-IP's, LNCaP whole cell lysates were washed with cold PBS and lysed using buffer K (20mM phosphate buffer, 0.15M NaCl, 0.1% NP40, 5mM EDTA, 0.6g/100mL CHAPS, containing phosphatase and protease inhibitors). The supernatant was collected after centrifugation at 10,000*g* for 10 min and the immunoprecipitation was performed overnight at 4°C with 5 µg each of anti-mTOR or AR rabbit antibody or a control anti-rabbit IgG antibody (Sigma-Aldrich). The next day, Protein sepharose™ 4 fast flow (GE Healthcare) beads were added for 3 h; beads were washed five times with buffer K prior to the addition of 50 µl of 1x Laemmli buffer. IP'd samples were incubated for 10 min at 95°C before

Western blotting analysis. For mTOR visualization on Western Blot following co-IP, LNCaP whole cell lysates were washed with cold PBS and lysed in RIPA buffer (Tris pH7.5, 2 mM EDTA, 2 mM EGTA, 0.5 M mannitol, 1% triton, containing phosphatase and protease inhibitors). The supernatant was collected after centrifugation at 10,000*g* for 15 min and the immunoprecipitation was performed overnight at 4°C with 3 µg each of anti-mTOR or AR rabbit antibody or a control anti-rabbit IgG antibody (Sigma-Aldrich), using Novex Dynabeads® (Life Technologies™). After three washes with 1x TBS, 40 µl of 1x Laemmli buffer was added and incubated for 5 min at 95°C before Western blotting analysis.

Human tissues and clinical datasets analyses

Reported studies on mTOR in human tissues made use of diverse methods and antibodies to assess its expression and distribution. Our IHC method was optimized by systematically testing parameters (antigen retrieval, protein blocking, concentrations of primary, secondary and DAB) to ensure high specificity of staining and negligible background. Negative controls consisted in omission of primary antibodies and also competition of antibody binding to the protein in tissue sections by adding different quantities of the peptide antigen used to produce mTOR (antibody: Ab32028 and synthetic peptide: Ab193663; Abcam). For validation of nuclear staining in a few patient tissues, the mTOR and P-mTOR antibodies available from Cell Signaling Technology (2983 and 2971) were used at concentrations of 1/400 and 1/100, respectively. IHC was performed on FFPE blocks cut to obtain 4 µm sections on positively charged microscope slides. Sections were dewaxed with xylene and rehydrated progressively in alcohol (100%, 90%, 70%) and distilled water. Sections were washed with Tris buffer saline (TBS), pH 7.2 for the remaining steps. Tissue sections were antigen retrieved in 0.2 M citrate buffer, pH 6.0, in a pressure cooker, heated in a microwave for 12 min, followed by 15 min of ice cooling at room temperature. Endogenous peroxidase blocking was performed using a 30% hydrogen peroxide solution (Leica Biosystem Inc, Canada) for 20 min. Sections were then immersed for an additional 30 min in a protein blocking reagent consisting of normal goat serum in PBS containing carrier protein (EMD Millipore, ON, Canada) prior to staining. Slides were next incubated overnight in a refrigerator (5-7°C) with the primary mTOR Abs (dilution of stock solution). Following three washes with TBS-Tween, bound Abs were detected using a Biotinylated secondary antibody (Goat anti-Rabbit IgG, and anti-Mouse IgG) "ready-to-use" for 45 min incubation (EMD Millipore, ON, Canada). The amplification was done using the streptavidin horseradish peroxidase (HRP) enhancer for 15 min, according to the manufacturer's instructions (EMD Millipore, ON, Canada). Immunoreactivity was visualized by Histofine DAB-3S Kit (Nichirei Biosciences, Tsukiji, Chuo-ku, Tokyo, Japan.) Sections were counterstained with Hematoxylin.

The reactivity of tissues to mTOR Abs was assessed at 20x magnification following the scanning of stained sections with the Aperio Digital Pathology Scanner (at least 500 cells/core). The image analyses were done with the e-slide Manager software by applying a nuclear staining quantification algorithm (nuclear v9) to determine H-score. After setting up the parameters for the ePathology algorithm, the staining intensity was recorded in each compartment on a scale

from 0 to 3 (0+ negative, 1=weak, 2=moderate, 3=strong) and expressed quantitatively by H Score = Σ (Pi(i)) X100, where *i* is the intensity of staining, and Pi the percentage of cells for each intensity; "X100" gives a value between 0-300 (Detre et al. 1995). Assessments were performed blindly by two viewers and approved by a genito-urinary (GU)-pathologist. Average H Score values were analysed in benign cells of glands and in tumor cells among disease stages (i.e. from localized to advanced disease) and within disease stages (i.e. rising Gleason Scores within localized disease).

To obtain the mTOR-targeted 24-gene signature, clustering analysis was performed using both the Lapointe et al. (Lapointe et al. 2004) and Tomlins et al. (Tomlins et al. 2007) cohorts, to select genes with the strongest classifying capacity to discriminate between primary tumors and lymph node metastases or metastatic CRPC, respectively. Only genes with strong clustering weights in both cohorts and associated with similar expression patterns between primary tumors and aggressive PCa were kept. The Taylor et al. (Taylor et al. 2010) cohort was used as a training set, and the 24-gene signature was based on the sum of increased or decreased expression compared to the median of each gene and then subdivided into three categories (protective, intermediate, and aggressive signatures). This 24-gene signature was then applied to the provisional TCGA prostate adenocarcinoma cohort (data from April 2017)(Cerami et al. 2012; Gao et al. 2013). A schematic illustrating the how the mTOR-targeted genes lists were derived is depicted in Figure S6H.

Supplemental References

Cerami E, Gao J, Dogrusoz U, Gross BE, Sumer SO, Aksoy BA, Jacobsen A, Byrne CJ, Heuer ML, Larsson E et al. 2012. The cBio cancer genomics portal: an open platform for exploring multidimensional cancer genomics data. *Cancer Discov* **2**: 401-404.

Chaveroux C, Eichner LJ, Dufour CR, Shatnawi A, Khoutorsky A, Bourque G, Sonenberg N, Giguere V. 2013. Molecular and genetic crosstalks between mTOR and ERRα are key determinants of rapamycin-induced non-alcoholic fatty liver. *Cell Metab* **17**: 586-598.

Detre S, Saclani Jotti G, Dowsett M. 1995. A "quickscore" method for immunohistochemical semiquantitation: validation for oestrogen receptor in breast carcinomas. *J Clin Pathol* **48**: 876-878.

Gao J, Aksoy BA, Dogrusoz U, Dresdner G, Gross B, Sumer SO, Sun Y, Jacobsen A, Sinha R, Larsson E et al. 2013. Integrative analysis of complex cancer genomics and clinical profiles using the cBioPortal. *Sci Signal* **6**: pl1.

Gravina GL, Marampon F, Petini F, Biordi L, Sherris D, Jannini EA, Tombolini V, Festuccia C. 2011. The TORC1/TORC2 inhibitor, Palomid 529, reduces tumor growth and sensitizes to docetaxel and cisplatin in aggressive and hormone-refractory prostate cancer cells. *Endocr Relat Cancer* **18**: 385-400.

Lapointe J, Li C, Higgins JP, van de Rijn M, Bair E, Montgomery K, Ferrari M, Egevad L, Rayford W, Bergerheim U et al. 2004. Gene expression profiling identifies clinically relevant subtypes of prostate cancer. *Proc Natl Acad Sci U S A* **101**: 811-816.

Mehrian-Shai R, Chen CD, Shi T, Horvath S, Nelson SF, Reichardt JK, Sawyers CL. 2007. Insulin growth factor-binding protein 2 is a candidate biomarker for PTEN status and

PI3K/Akt pathway activation in glioblastoma and prostate cancer. *Proc Natl Acad Sci U S A* **104**: 5563-5568.

Sun Y, Wang BE, Leong KG, Yue P, Li L, Jhunjhunwala S, Chen D, Seo K, Modrusan Z, Gao WQ et al. 2012. Androgen deprivation causes epithelial-mesenchymal transition in the prostate: implications for androgen-deprivation therapy. *Cancer Res* **72**: 527-536.

Taylor BS, Schultz N, Hieronymus H, Gopalan A, Xiao Y, Carver BS, Arora VK, Kaushik P, Cerami E, Reva B et al. 2010. Integrative genomic profiling of human prostate cancer. *Cancer Cell* **18**: 11-22.

Tomlins SA, Mehra R, Rhodes DR, Cao X, Wang L, Dhanasekaran SM, Kalyana-Sundaram S, Wei JT, Rubin MA, Pienta KJ et al. 2007. Integrative molecular concept modeling of prostate cancer progression. *Nat Genet* **39**: 41-51.

Vlietstra RJ, van Alewijk DC, Hermans KG, van Steenbrugge GJ, Trapman J. 1998. Frequent inactivation of PTEN in prostate cancer cell lines and xenografts. *Cancer Res* **58**: 2720-2723.

Watson PA, Arora VK, Sawyers CL. 2015. Emerging mechanisms of resistance to androgen receptor inhibitors in prostate cancer. *Nat Rev Cancer* **15**: 701-711.

Wu X, Senechal K, Neshat MS, Whang YE, Sawyers CL. 1998. The PTEN/MMAC1 tumor suppressor phosphatase functions as a negative regulator of the phosphoinositide 3-kinase/Akt pathway. *Proc Natl Acad Sci U S A* **95**: 15587-15591.